

Collision-Induced Light Scattering in Gases.

I. The Rare Gases: Ar, Kr, and Xe

J. P. McTague

*Science Center, North American Rockwell Corporation, Thousand Oaks, California 91360
and Department of Chemistry, University of California,* Los Angeles, California 90024*

and

George Birnbaum

Science Center, North American Rockwell Corporation, Thousand Oaks, California 91360

(Received 14 August 1970)

Gaseous Ar, Kr, and Xe are observed at room temperature to scatter light into a broad frequency band whose intensity varies as the square of the density at low densities. Such scattering is attributed to an incremental polarizability due to the distortion of the electronic distributions of colliding atoms. Studies of the depolarization ratio show that the collision-induced spherical polarizability is negligible with respect to the induced anisotropy. Within experimental error, the (relative) integrated depolarized intensity at low densities and the second virial Kerr coefficient, to which it is directly related, are in agreement. Studies made at wave-number deviations of about $5 - 100 \text{ cm}^{-1}$ from the laser frequency show that the spectral shape is exponentiallike and the bandwidth is of the order of the duration of collision.

1. INTRODUCTION

It has been known for a long time that there is a slight depolarization of the light scattered elastically in liquids¹ and gases² consisting of spherical molecules. Such results are anomalous if one regards the fluid as being composed of isolated, non-interacting spherical molecules. However, rather recently Buckingham and Stephen,³ Kielich,^{4,5} and Theimer and Paul⁶ have theoretically shown that such scattering can occur if account is taken of the fact that the polarizability is changed as a result of the interaction between the dipole moments induced by the applied field. This interaction induces an effective anisotropic polarizability in interacting spherical molecules, and anisotropic scattering results. Thibeau, Oksengorn, and Vodar^{7,8} demonstrated depolarized scattering from Ar by making measurements of scattered intensity as a function of pressure up to 800 bar.

The experimental and theoretical work mentioned thus far have dealt with the integrated intensity of gases composed of spherical molecules, and the question of the spectral distribution of scattered light did not arise. Levine and Birnbaum,⁹ however, considered this question, and derived on the basis of a highly idealized model the spectrum of depolarized light for gases at low densities where binary collisions predominate. They predicted that the intensity in the wings of both the polarized and depolarized lines should decrease essentially exponentially with increasing frequency deviation from the incident radiation. McTague and Birnbaum,¹⁰ using a laser to illuminate the sample and a monochromator to analyze the spectral distribution of the scattered light, obtained the line shape for gas-

eous Ar and Kr and confirmed the essentially exponential line wings, as well as the dependence of the scattered light intensity on the square of the density at sufficiently low densities.

This paper gives a full account of this experiment, and includes improved measurements on Ar and Kr and new results¹¹ on Xe. The integrated intensity of the depolarized spectrum is compared with the second Kerr virial coefficient¹² to which it is directly related,⁵ and with calculations which have been made of the induced polarizability based on the point-dipole model.¹² Although we consider the spectral shape of the scattered radiation, a treatment of this problem will be presented elsewhere.¹³

II. THEORETICAL CONSIDERATIONS

The phenomenon of Rayleigh scattering by atoms and spherical molecules in gases is well known. For monochromatic incident radiation, this scattered light is Doppler broadened by the thermal motion of the atoms and produces a line with a width at room temperature of the order of 0.1 cm^{-1} for visible light. However, during a collision the electronic distribution of the colliding atoms is distorted by interatomic interactions producing a polarizability in the colliding complex which differs from the sum of the polarizabilities of the separated atoms. This incremental polarizability is anisotropic and scatters depolarized radiation into a band whose half-width is typically of the order of 10 cm^{-1} , a value determined essentially by the duration of collision. This type of scattering differs markedly from the usual Rayleigh scattering not only in that the scattered radiation is depolarized and its bandwidth is very much greater, but also in the fact that at low den-

sities the intensity of the scattered light varies as the square of the density rather than linearly.

Scattering from the polarizability increment can be thought of from two points of view. On the one hand, it can be viewed as Rayleigh scattering by the time-varying polarizability induced in colliding atoms. On the other hand, it can be thought of as Raman scattering involving a change in the translational state of the relative motion of atoms. In the latter point of view, the frequency shift $\Delta\omega$ of the scattered light is related to the relative velocities of a pair of colliding atoms before and after collision, v and v' , by the Bohr energy condition

$$\hbar\Delta\omega = \frac{1}{2}m(v^2 - v'^2),$$

where m is the reduced mass.

A. General Relations

Expressions suitable for analyzing the experimental results can be obtained from the formalism developed by Ben-Reuven and Gershon.¹⁴ Consider first a beam of light scattered by a homogeneous isotropic fluid consisting of nonspherical molecules. Let E_i , \hat{n}_i , \hat{k}_i , and ω_i be, respectively, the electric field amplitude, polarization unit vector, propagation vector, and frequency of the incident beam. Consider the scattered light propagating in the direction \hat{k}_s , and let the detector be located at a distance R_0 from an arbitrary reference point in the sample. The frequency distribution $\omega = \omega_s - \omega_i$ of the scattered light is

$$I(\omega) = \frac{1}{2\pi} \int_{-\infty}^{\infty} J(t) e^{-i\omega t} dt, \quad (1)$$

where

$$J(t) = C\rho\epsilon^{-2} \langle \sum_B [\hat{n}_s \cdot \underline{\alpha}(B; t) \cdot \hat{n}_i] [\hat{n}_s \cdot \underline{\alpha}(A; 0) \cdot \hat{n}_i] \times \exp[i\hat{k} \cdot \{\vec{r}(B; t) - \vec{r}(A; 0)\}] \rangle \quad (2)$$

and

$$C = V k_i^4 I_i (4\pi R_0)^{-2}. \quad (3)$$

Here $\underline{\alpha}(B; t)$ is the polarizability tensor in the laboratory frame of molecule B at time t ; $\underline{\alpha}(A; 0)$ is the polarizability of molecule A at time $t=0$; $I_i = cE_i^2/4\pi$ is the intensity of the incident light beam; $\vec{r}(B; t)$ is the separation of molecule B from the reference point in the sample at time t ; $\vec{r}(A; 0)$ is the separation of molecule A from the reference point at $t=0$; $\hat{k} = \hat{k}_s - \hat{k}_i$; and ϵ is the permittivity of the fluid at the applied frequency. The summation over molecule A has been replaced in (2) by ρV times a thermal average, denoted by the angular brackets, over all positions and orientations. Here V is the scattering volume and ρ is the number of molecules per cm^3 .

Since the wavelength of light is very much greater

than the range of molecular correlations of interest here, the exponential in (2) is replaced by unity. Another important simplification is to consider only self-correlations, and not the correlation of molecule A with all other molecules B . We therefore replace B by A and drop the summation over B in (2). Using the methods of tensor algebra, Ben-Reuven and Gershon¹⁴ separate all geometrical from molecular factors in the correlation function. If one defines

$$F(t) = J(t)(\epsilon^2/C\rho),$$

their result with the above simplifications, but generalized here to allow for a time-dependent polarizability, is

$$F(t) = F_{00}^0(t)\phi_{00}^0 + F_{22}^0(t)\phi_{22}^0, \quad (4)$$

where

$$F_{00}^0(t) = 3 \langle \alpha(0)\alpha(t) \rangle, \quad (5)$$

$$\phi_{00}^0 = \frac{1}{3}(\hat{n}_i \cdot \hat{n}_s)^2, \quad (6)$$

$$F_{22}^0(t) = \frac{2}{3} 5^{-1/2} \langle \beta(0)\beta(t)P_2(x) \rangle, \quad (7)$$

$$\phi_{22}^0 = [6(5^{1/2})]^{-1} [3 + (\hat{n}_i \cdot \hat{n}_s)^2]. \quad (8)$$

The function $P_2(x)$, where $x = \cos\theta(t)$, is the Legendre polynomial

$$P_2(x) = \frac{1}{2}[3\cos^2\theta(t) - 1].$$

The molecules are assumed to be axially symmetric so that

$$\alpha = \frac{1}{3}(\alpha_{\parallel} + 2\alpha_{\perp}), \quad (9)$$

$$\beta = \alpha_{\parallel} - \alpha_{\perp}, \quad (10)$$

where α_{\parallel} and α_{\perp} are, respectively, the polarizability parallel and perpendicular to the symmetry axis. The angle $\theta(t)$ is the angle of the molecular axis at time t relative to that at $t=0$. Then (5)–(8) give

$$F(t) = \langle \alpha(0)\alpha(t) \rangle (\hat{n}_i \cdot \hat{n}_s)^2 + \langle \beta(0)\beta(t)P_2(x) \rangle \{ (45)^{-1} [3 + (\hat{n}_i \cdot \hat{n}_s)^2] \}. \quad (11)$$

Similar results have been presented by Gordon.¹⁵

These results may be extended to a pair of interacting atoms or spherical molecules by regarding the interacting pair as an axially symmetric molecule whose polarizability is a function of the internuclear separation r . We let $\alpha(r)$ and $\beta(r)$, which are functions of time through the intermolecular distance $r(t)$, represent the incremental polarizabilities defined by

$$\alpha(r) = \frac{1}{3}[\alpha_{\parallel}(r) + 2\alpha_{\perp}(r)] - 2\alpha, \quad (12)$$

$$\beta(r) = \alpha_{\parallel}(r) - \alpha_{\perp}(r). \quad (13)$$

In these equations $\alpha_{\parallel}(r)$ and $\alpha_{\perp}(r)$ are the parallel and perpendicular polarizabilities of a pair of interacting atoms, considered as one axially symmet-

ric molecule, and α is the polarizability of a single isolated atom. Although these equations show that $\alpha(r)$ and $\beta(r)$ may be positive or negative, the sign plays no essential role in the present experiment, which measures $\langle \alpha^2(r) \rangle$ and $\langle \beta^2(r) \rangle$. To convert (2) into a form applicable to the spectrum of light scattered by molecular pairs of the same species, we need only replace the density ρ by $\frac{1}{2} V \rho^2$ to obtain

$$J(t) = \frac{V^2 \rho^2 k_1^4 I_i}{(4\pi R_0)^2 2\epsilon^2} F(t), \quad (14)$$

where $F(t)$ is given by (11) and the polarizabilities given therein are defined by (12) and (13).

In the experiment we use right-angle scattering with the geometry defined by a coordinate system with the y axis parallel to the direction of propagation of the incident light and the x axis parallel to that of the scattered light. For the case that the detector measures both the y and z polarized components of the scattered radiation, we obtain from (11)

$$F_y(t) = \langle \alpha(0)\alpha(t) \rangle + \frac{7}{45} \langle \beta(0)\beta(t)P_2(x) \rangle, \quad (15)$$

$$F_z(t) = \frac{2}{15} \langle \beta(0)\beta(t)P_2(x) \rangle, \quad (16)$$

where the subscripts x and z refer to the direction of polarization of the incident light. The spectral distribution of the scattered intensity is then

$$I_\eta(\omega) = \frac{CV\rho^2}{4\pi\epsilon^2} \int_{-\infty}^{\infty} F_\eta(t) e^{-i\omega t} dt, \quad (17)$$

where $\eta = x$ or z . It is convenient to define the Fourier transforms

$$\int_{-\infty}^{\infty} \langle \alpha(0)\alpha(t) \rangle e^{-i\omega t} dt = A(\omega), \quad (18)$$

$$\int_{-\infty}^{\infty} \langle \beta(0)\beta(t)P_2(x) \rangle e^{-i\omega t} dt = B(\omega). \quad (19)$$

The depolarization ratio defined by

$$D(\omega) = I_x(\omega)/I_z(\omega) \quad (20)$$

is then from (18) and (19)

$$D(\omega) = \frac{\frac{2}{15}B(\omega)}{A(\omega) + \frac{7}{45}B(\omega)}. \quad (21)$$

B. Integrated Intensity

Equation (17) provides a complete description of the experiment at low densities if the correlation functions $F_\eta(t)$ are known. However, important information can be obtained from the integrated intensity

$$I = \int_{-\infty}^{\infty} I(\omega) d\omega = J(0), \quad (22)$$

which is simply related to quantities of interest. Thus, using (15) to (17), one obtains¹⁶

$$I_x = \frac{C\rho^2 V}{2\epsilon^2} [\langle \alpha^2(r) \rangle + \frac{7}{45} \langle \beta^2(r) \rangle], \quad (23)$$

$$I_z = \frac{C\rho^2 V}{2\epsilon^2} \frac{2}{15} \langle \beta^2(r) \rangle, \quad (24)$$

with

$$V \langle \beta^2(r) \rangle = 4\pi \int_0^\infty \beta^2(r) g(r) r^2 dr \quad (25)$$

and a similar relation for $V \langle \alpha^2(r) \rangle$. Here $g(r)$ is the radial distribution function which for gases at low density is given by

$$g(r) = \exp[-V(r)/kT], \quad (26)$$

where $V(r)$ is the intermolecular potential. The depolarization ratio from (23) and (24) is

$$D = \frac{\frac{2}{15} \langle \beta^2(r) \rangle}{\langle \alpha^2(r) \rangle + \frac{7}{45} \langle \beta^2(r) \rangle}. \quad (27)$$

It is clear that, in general, D and $D(\omega)$ may differ.

In investigating the Kerr constant of gases composed of atoms or spherical molecules, Buckingham and Dunmur¹² found a density-squared dependence which they interpreted as arising from the induced anisotropic polarization in molecular pairs. This contribution is characterized by the second Kerr virial coefficient

$$B_K = \frac{8\pi^2 N_0^2}{405kT} \int_0^\infty \beta_0(r)\beta(r)g(r)r^2 dr, \quad (28)$$

where N_0 is Avogadro's number and $\beta_0(r)$ and $\beta(r)$ are, respectively, the optical and static values of the polarizability anisotropy. Unless the laser frequency is close to an atomic transition, it is usually sufficiently accurate to take $\beta_0(r) = \beta(r)$. Then, comparing (24) and (28), we see that

$$I_x^{(2)}/B_K = 27CkT/2\pi\epsilon^2 N_0^2; \quad (29)$$

i. e., the depolarized intensity (integrated over the entire band) $I_x^{(2)} = I_x/\rho^2$ is directly proportional to the second Kerr virial coefficient.⁵ As far as we know, there is no experiment other than the one discussed here which measures $\langle \alpha^2(r) \rangle$, although the second dielectric virial coefficient measures $\langle \alpha(r) \rangle$.¹⁷

To understand how the polarizability of a spherical molecule changes due to its interaction with neighboring spherical molecules, one considers the induced dipole moment in a given molecule due to the applied field \vec{E} and the internal field \vec{F} due to all the surrounding molecules,

$$\vec{M} = \alpha(\vec{E} + \vec{F}). \quad (30)$$

In the dipolar approximation, where it is assumed that the applied electric field induces a point dipole in a given molecule which then induces point dipoles in neighboring molecules, one obtains from (30) for a pair of molecules¹⁸

$$\alpha(r) = 4\alpha^3 r^{-6}, \quad (31)$$

$$\beta(r) = 6\alpha^2 r^{-3}. \quad (32)$$

To evaluate $\langle \alpha^2(r) \rangle$ and $\langle \beta^2(r) \rangle$, we use the Lennard-Jones potential for $V(r)$ in (26) to obtain

$$V\langle \alpha^2(r) \rangle = 16\pi\alpha^6 H_{12}(y)/3y^4\sigma^9, \quad (33)$$

$$V\langle \beta^2(r) \rangle = 12\pi\alpha^4 H_6(y)/y^4\sigma^3, \quad (34)$$

$$y = 4\epsilon/kT,$$

where σ and ϵ are the Lennard-Jones parameters, and $H_n(y)$ are tabulated functions.¹⁹

III. EXPERIMENTAL ARRANGEMENT AND RESULTS

Right-angle scattering was observed using as the exciting source the 5145-Å line of a Coherent Radiation Laboratories model 52 argon ion laser with an output power of about 0.4 W. Spectral analysis and detection were accomplished with a Spex model 1400 double monochromator and a cooled ITT FW 130 photomultiplier with a dark count of 0.4 sec⁻¹.

In order to display the line shape most clearly, spectra were recorded from the logarithmic output of a photon count rate meter. The frequency was scanned at approximately 2 Å/min. Typical scans of the depolarized radiation scattered from compressed Ar, Kr, and Xe are shown in Figs. 1-3.

The density dependence of the intensity at a given wavelength was determined by counting photoelectron pulses for approximately 10 min, then increasing the density and repeating. It was found necessary to allow at least 30 min after each change of pressure for thermal equilibration.

In order to study the polarization properties of the scattered light, the incident beam was rotated using a half-wave plate. In order to maximize the observed signal, the polarization of the scattered beam was not analyzed. For isotropic systems such as gases, such analysis would add no new information.

IV. DISCUSSION OF EXPERIMENTAL RESULTS

A. Density Dependence

The density dependence of the intensity of the scattered light for Ar, Kr, and Xe was investigated at a number of frequencies for the x and z polarizations. The results for two frequencies are shown in Figs. 4-6, where the intensity per unit density is plotted as a function of density. In the limit that $\rho \rightarrow 0$, the intensity varies as ρ^2 , indicating that the scattering is due to atomic pairs. Departure from a ρ^2 dependence may be seen at the higher densities, and over the density range measured may be represented by a component of the intensity which varies as ρ^3 . Thus the density dependence of the scattered light at low densities may be represented by

$$I_\eta(\omega) = \rho^2 I_\eta^{(2)}(\omega) - \rho^3 I_\eta^{(3)}(\omega), \quad (35)$$

where $\eta = x$ or z is the direction of polarization of the incident light, and the x axis points from the scatterer to the detector. The lack of data at densities less than 30 amagats for Ar at 20 cm⁻¹ does not allow us to distinguish between the two curves fitted to the data for Ar at 20 cm⁻¹ in Fig. 4.^{19a}

The coefficient of the ρ^3 term may be attributed to interactions of three atoms, the negative sign indicating that there is a destructive interference. From Figs. 4-6 one observes that, at a given frequency, the three-body term which manifests itself in the curvature of I/ρ versus ρ increases in the order Ar-Kr-Xe, as one might expect. Furthermore, the three-body term is seen to be relatively more important at the lower frequency. On a quantitative basis, at a frequency deviation of 20 cm⁻¹, $-I_x^{(3)}/I_x^{(2)}$ is 1.3, 4.0, and 5.6×10^{-3} amagat⁻¹ for Ar, Kr, and Xe, respectively. At 40-cm⁻¹ deviation, $I_x^{(3)}/I_x^{(2)} = 0$, within experimental error.

The effect of destructive interference in three-body interactions has been observed in collision-induced absorption arising from interacting quad-

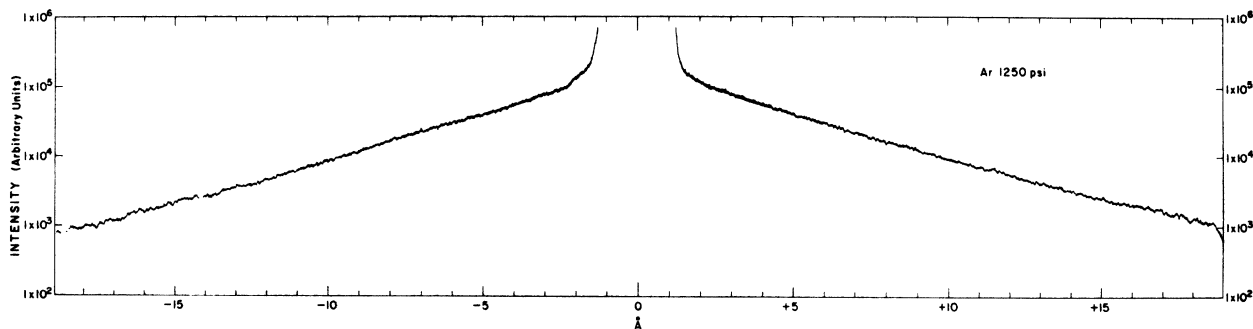


FIG. 1. Spectrum of depolarized light scattered from Ar at 1250 lb/in.². Wavelength of incident radiation is 5145 Å. Note that $\delta\nu/\delta\lambda = -3.78 \text{ cm}^{-1}/\text{Å}$ at 5145 Å.

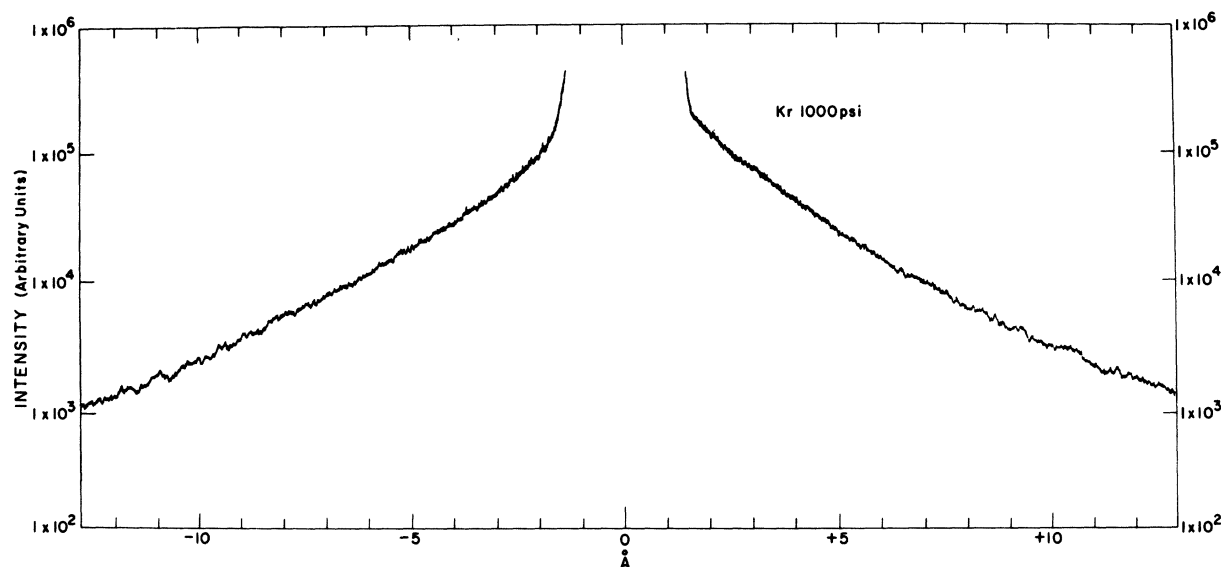


FIG. 2. Spectrum of depolarized light scattered from Kr at 1000 lb/in.². Wavelength of incident light is 5145 Å. Note that $\delta\nu/\delta\lambda = -3.78 \text{ cm}^{-1}/\text{Å}$ at 5145 Å.

rupoles.^{20,21} The reduction in the collision-induced intensity compared with the intensity expected on the basis of just two-body interactions becomes much more pronounced in the liquid state as shown by measurements on induced light scattering in liquid Ar,²² as well as induced absorption in liquid CO₂.²³

B. Depolarization Ratio

The depolarization ratio is 0.86 ± 0.04 for Ar, Kr, and Xe at 10 and 15 cm⁻¹ from the laser frequency. This result is in agreement with (21) if the polarized component of the scattered radiation, $A(\omega)$, is negligible compared with the depolarized component, $B(\omega)$. To show that this is the case, we estimate $\langle\alpha^2\rangle/\langle\beta^2\rangle$. It is permissible to work

with $\langle\alpha^2\rangle/\langle\beta^2\rangle$ rather than $A(\omega)/B(\omega)$ because $D(\omega)$ was found to be a weak function of frequency. On the basis of the point-dipole model, i. e., (33) and (34), we obtain

$$\frac{V\langle\alpha^2(r)\rangle}{V\langle\beta^2(r)\rangle} = \frac{4\alpha^2 H_{12}(y)}{\sigma^6 H_6(y)}. \quad (36)$$

For rare gases at room temperature, one has $y \sim 2$, and $H_{12}(2)/H_6(2) \approx 0.4$. Then since $\alpha \ll \sigma^3$ (for Ar, for example, $\alpha/\sigma^3 \approx 3 \times 10^{-2}$), $V\langle\alpha^2(r)\rangle$ as given in (33) is a completely negligible quantity, and (27) reduces to $\frac{5}{7} = 0.857$, in agreement with experiment.

C. Integrated Intensity

Table I gives the integrated intensity $I_x^{(2)}$ normalized to the values for Ar, since we do not de-

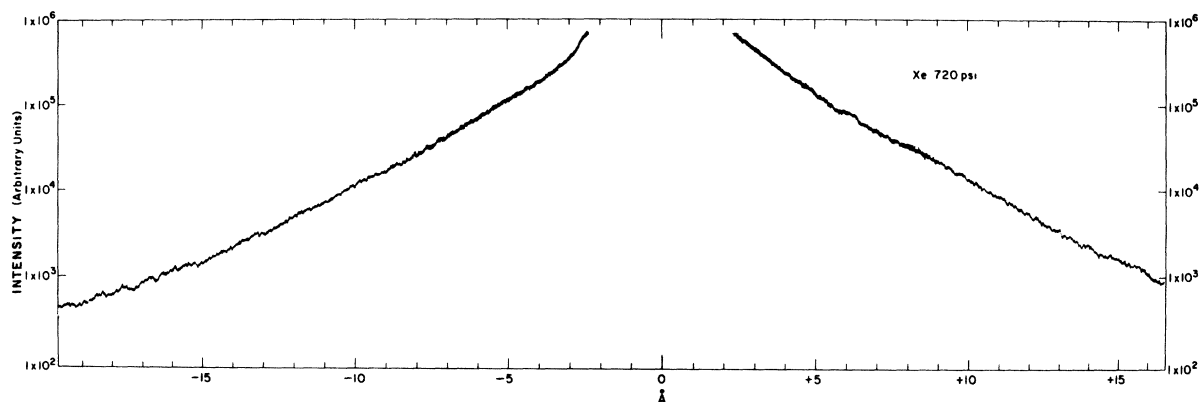


FIG. 3. Spectrum of depolarized light scattered from Xe at 720 lb/in.². Wavelength of incident light is 5145 Å. Note that $\delta\nu/\delta\lambda = -3.78 \text{ cm}^{-1}/\text{Å}$ at 5145 Å.

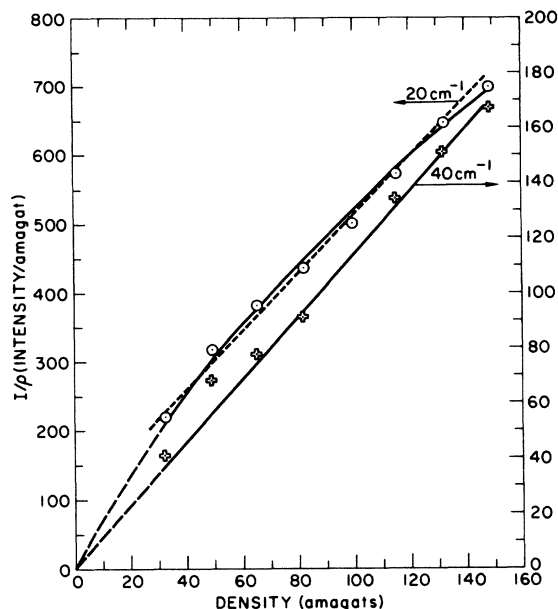


FIG. 4. Density dependence of the depolarized light scattered from Ar.

termine the absolute intensity. To obtain the integrated intensity, we extrapolated the observed spectrum to the origin on the assumption that it follows an exponential shape. We feel that the major source of error in the relative integrated intensity is due to the lack of knowledge of the true line shape in the region near the laser frequency. However, a very crude estimate based on the arbitrary assumption that the spectrum in this region is not exponential, but becomes constant in intensity, leads us to assume an error of very roughly 15%. Also shown in Table I is the second Kerr virial coefficient B_K determined experimentally and calculated on the basis of the point-dipole model, namely, (34). Within the combined experimental errors, the normalized values of $I_x^{(2)}$ and B_K are seen to agree. In all cases, $B_K(\text{calc}) > B_K(\text{expt})$, the discrepancy increasing with the mass of the rare gas.

The deficiency of the point-dipole model has already been noted in measurements of the second dielectric virial coefficient where negative values of $\langle \alpha(r) \rangle$ were obtained for the light rare gases He and Ne,¹⁷ an impossible result on the basis of (31). For Ar and Kr, the measured values of $\langle \alpha(r) \rangle$ are positive but significantly less than the values computed from (31). These facts clearly mean that there must be a negative contribution to $\alpha(r)$ and $\beta(r)$, and that $\alpha_{11}(r) - 2\alpha$ and $\alpha_1(r) - 2\alpha$ have opposite signs over the important part of the interaction.²⁴ To gain some insight into such results, DuPré and McTague²⁵ calculated the polarizability tensor as a function of internuclear separation of

two interacting hydrogen atoms in the nonbonding triplet state and found that there is a substantial contribution both to $\alpha(r)$ and $\beta(r)$ arising from the overlap interaction, and that they have signs opposite to those of the long-range dispersion contributions.

D. Line Shape

In Figs. 1, 2, 3 we show in a semilogarithmic presentation the spectral line shape for the depolarized light scattered by Ar, Kr, and Xe, respectively. The Rayleigh peak in the region of zero frequency deviation is not shown and is approximately 10^3 – 10^4 times more intense than the collision-induced spectrum. The spectra are shown only up to the point where the logarithmic amplifier became nonlinear in its response.

The negative frequency or Stokes side of the spectra corresponds to an inelastic collision of a photon with a pair of interacting atoms in which the atoms separate with greater relative kinetic energy and the scattered radiation is shifted to a lower frequency. The anti-Stokes side corresponds to the inverse process. It has been verified that the ratio of the Stokes to anti-Stokes intensities is equal to the Boltzmann factor $\exp(\hbar\omega/kT)$, where ω is the frequency shift.

As with collision-induced absorption, several things can be said at the outset about collision-in-

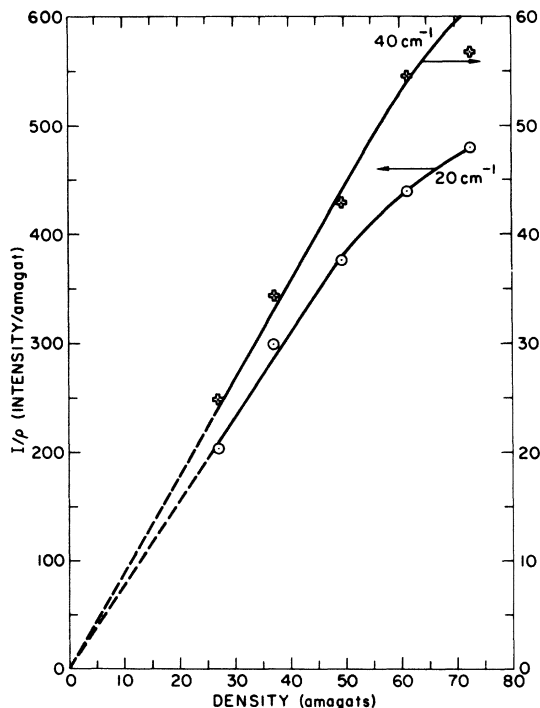


FIG. 5. Density dependence of the depolarized light scattered from Kr.

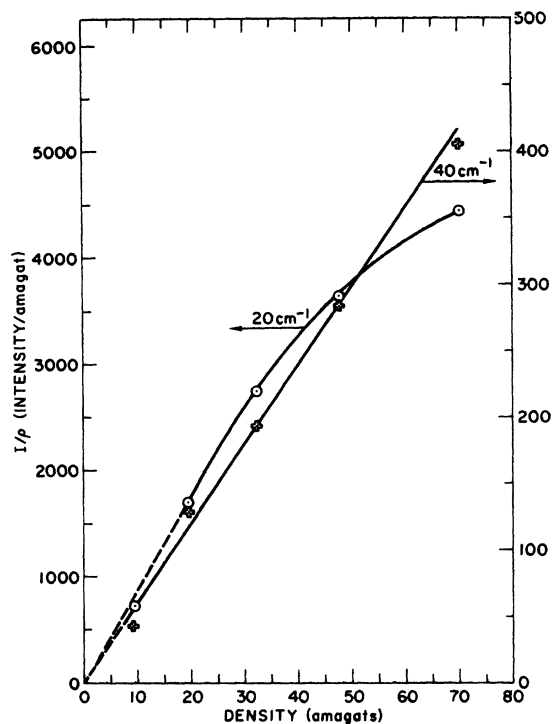


FIG. 6. Density dependence of the depolarized light scattered from Xe.

duced light scattering, provided bimolecular collisions predominate and the contribution of dimers is not significant. Then, since the light scattering persists only during a collision, the width of the collision-induced band is from the uncertainty principle given in order of magnitude by

$$\Delta\omega \sim v/r_0 \quad (37)$$

Here v is the mean relative velocity, and r_0 is the range of the interaction, which for long-range interactions is of the order of the kinetic diameter. Furthermore, the shape of the band is independent of density, although the intensity at each wavelength should vary as the square of the density at suffi-

ciently low densities.

The first attempt to derive a line shape for collision-induced light scattering is due to Levine and Birnbaum,⁹ who supposed that the induced polarizability varies with interatomic separation as a Gaussian function whose width is essentially the duration of collision. Then, assuming straight-line paths and considering the atoms as point particles, they were able to obtain a simple analytic result after averaging over all types of collisions. Although the parameters in the line shape are not directly related to those of real gases, the assumption of Gaussian pulses of induced polarizability is not unrealistic and their prediction of an exponential-like shape in the wings has been confirmed experimentally.^{10,11,26}

Thibeau and Oksengorn²⁷ have made a more detailed calculation of collision-induced light scattering, adopting the model of induction by a point dipole. Assuming straight paths, they divided the calculation into two contributions: one coming from the glancing collisions and the other from contact collisions. Since they assumed a single mean relative velocity instead of performing a machine calculation to average the two contributions over the Maxwell-Boltzmann distribution, it is not clear just what the final shape would be. However, we would not be surprised if this model gave an exponential-like dependence.

From the experiment we find that the line shape may be represented approximately by

$$\int_{-\infty}^{\infty} dt \langle \beta(0)\beta(t) P_2(x) \rangle e^{-i2\pi\nu t} = \sum_n B_n e^{-\nu/\Delta\nu_n} \quad (38)$$

where ν is the frequency deviation from the laser frequency in cm^{-1} , B_n is an intensity factor, and from (37),

$$\Delta\nu_n \sim v/2\pi cr_n \quad (39)$$

Although a single exponential represents roughly the observed spectrum, the data indicates that the far wings fall off somewhat more slowly than the near wings. Fitting the data at 20 and 40 cm^{-1}

TABLE I. Integrated depolarized intensity $I_x^{(2)} \propto \langle \beta^2 \rangle$ and second Kerr virial coefficient B_K .

Gas	$10^{24}\alpha$ (cm^3)	ϵ/k^2 ($^\circ\text{K}$)	$10^8\sigma^2$ (cm)	$\langle \beta^2 \rangle^b$ relative to Ar	$10^{12}B_K$ (esu) expt ^c	$10^{12}B_K$ (esu) theor ^d	B_K (theor) ^d relative to Ar	B_K (expt) relative to Ar
Ar	1.642 ^e	119.8	3.405	1	4.1 ± 0.61	5.6	1	1
Kr	2.484 ^e	171	3.60	2.6	16 ± 14	26	4.6	3.9
Xe	4.405 ^f	221	4.100	21	65 ± 22	140	25	16

^aJ. O. Hirschfelder, C. F. Curtiss, and R. B. Bird, *Molecular Theory of Gases and Liquids* (Wiley, New York, 1964), Table I-A, p. 1110. Force constants from second virial coefficients.

^b25 $^\circ\text{K}$.

^cReference 12. 23 $^\circ\text{K}$.

^dCalculated in Ref. 12 on the basis of the induced dipole model.

^eReference 17.

^fA. Dalgarno and A. E. Kingston, Proc. Roy. Soc. (London) **A259**, 424 (1960).

by a single exponential, we find, as shown in Table II, that (39) gives values of $\Delta\nu$ consistently greater than experiment. However, the ratios of experimental to theoretical linewidths are roughly constant, suggesting that (39) may be roughly valid to within a multiplicative constant. However, some caution must be exercised in drawing conclusions based on the observed spectral line shape, since in general one would expect the shape of the spectrum of light scattered by dimers to differ from that from colliding pairs of atoms. As shown by Levine,²⁸ there is a significant contribution to the integrated intensity by bound states of atomic pairs, i.e., dimers. At room temperature, the fractional contribution of dimers is about 10% for Ar, 15% for Kr, and 25% for Xe.

V. CONCLUSIONS

This work has explored the spectral character of collision-induced light scattering in the rare gases where the phenomenon is exhibited in its simplest form. Indeed, any depolarized scattering in the rare gases at frequencies well removed from the laser frequency must be due to the collision-induced process. The study of such scattering

TABLE II. Linewidth parameter. $T = 25^\circ\text{C}$.

Gas	$10^4\nu$ (cm/sec)	$\Delta\nu(\text{expt})^a$ (cm^{-1})	$\Delta\nu(\text{calc})^b$ (cm^{-1})	$\frac{\Delta\nu(\text{expt})}{\Delta\nu(\text{calc})}$
Ar	5.64	14	8.8	1.6
Kr	3.89	9.1	5.7	1.6
Xe	3.11	7.5	4.0	1.9

^aObtained by fitting $\exp(-\nu/\Delta\nu)$ to the data obtained at frequency deviations of 20 and 40 cm^{-1} , and at a density of approximately 30 amagats.

^bCalculated from (39) with $r_n = \sigma$, where σ is obtained from Table I.

would seem to hold the promise of investigating atomic motions and interactions.

Note added in proof. We thank Dr. V. Volterra for suggesting that the Ar data at 20 cm^{-1} in Fig. 4 may be represented by a curve passing through the origin, which is consistent with his results²⁹ taken at 10 cm^{-1} . Such a curve is also consistent with our earlier results¹⁰ taken at 10 and 15 cm^{-1} .

ACKNOWLEDGMENT

The authors thank Dr. H. B. Levine for valuable discussions regarding many aspects of this work.

*Contribution No. 2666 from the Department of Chemistry.

¹D. H. Rank, *J. Opt. Soc. Am.* **37**, 798 (1947), and the reference cited therein; R. Gans, *Handbuch der Experimental Physik* (Akademische Verlagsgesellschaft, Leipzig, 1928), Vol. 19, p. 394.

²R. R. Rudder and D. R. Bach, *J. Opt. Soc. Am.* **58**, 1260 (1968), and Refs. 1-5 cited therein.

³A. D. Buckingham and M. J. Stephen, *Trans. Faraday Soc.* **53**, 884 (1957).

⁴S. Kielich, *Acta Phys. Polon.* **19**, 711 (1960).

⁵S. Kielich, *J. Chem. Phys.* **46**, 4090 (1967).

⁶O. Theimer and R. Paul, *J. Chem. Phys.* **42**, 2508 (1965).

⁷M. Thibeau, B. Oksengorn, and B. Vodar, *Compt. Rend.* **263**, B135 (1966).

⁸M. Thibeau, B. Oksengorn, and B. Vodar, *J. Phys. (Paris)* **29**, 287 (1968).

⁹H. B. Levine and G. Birnbaum, *Phys. Rev. Letters* **20**, 439 (1968).

¹⁰J. P. McTague and G. Birnbaum, *Phys. Rev. Letters* **21**, 661 (1968).

¹¹J. P. McTague and G. Birnbaum, *Bull. Am. Phys. Soc.* **14**, 344 (1969).

¹²A. D. Buckingham and D. A. Dunmur, *Trans. Faraday Soc.* **64**, 1776 (1968).

¹³H. B. Levine and G. Birnbaum (unpublished).

¹⁴A. Ben-Reuven and N. D. Gershon, *J. Chem. Phys.* **51**, 893 (1969).

¹⁵R. G. Gordon, *Advan. Magn. Resonance* **3**, 1 (1968); *J. Chem. Phys.* **42**, 3658 (1965).

¹⁶Treatments of the integrated intensity in collision-

induced light scattering are given in Refs. 3 and 5. See also S. Kielich, *J. Phys. (Paris)* **29**, 619 (1968); *J. Quantum Electron.* **QE-4**, 744 (1968).

¹⁷See, for example, R. H. Orcutt and R. H. Cole, *J. Chem. Phys.* **46**, 697 (1967).

¹⁸Equation (31) is given by A. D. Buckingham, *Trans. Faraday Soc.* **52**, 1035 (1956). Equation (32) is cited in Ref. 12 and attributed to L. Silberstein, *Phil. Mag.* **33**, 521 (1917). This equation has recently been obtained by H. B. Levine and D. A. McQuarrie, *J. Chem. Phys.* **49**, 4181 (1968).

¹⁹A. D. Buckingham and J. A. Pople, *Trans. Faraday Soc.* **51**, 1029 (1955).

^{19a}See Note added in proof.

²⁰A. A. Maryott and G. Birnbaum, *J. Chem. Phys.* **36**, 2026 (1962); **36**, 2032 (1962).

²¹G. Birnbaum, H. B. Levine, and D. A. McQuarrie, *J. Chem. Phys.* **46**, 1557 (1967).

²²J. P. McTague, P. A. Fleury, and D. B. DuPré, *Phys. Rev.* **188**, 303 (1969).

²³W. Ho, G. Birnbaum, and A. Rosenberg (unpublished).

²⁴H. B. Levine and D. A. McQuarrie, *J. Chem. Phys.* **49**, 4181 (1968).

²⁵D. B. DuPré and J. P. McTague, *J. Chem. Phys.* **50**, 2024 (1969).

²⁶W. S. Gornall, H. E. Howard-Lock, and B. P. Stoicheff, *Phys. Rev. A* **1**, 1288 (1970).

²⁷M. Thibeau and B. Oksengorn, *Mol. Phys.* **15**, 579 (1968).

²⁸H. B. Levine (unpublished).

²⁹V. Volterra, J. A. Bucaro, and T. A. Litovitz (unpublished).